

Nuclear resonance vibrational spectroscopic definition of peroxy intermediates in non-heme iron sites

Kyle D. Sutherlin,^a Lei V. Liu,^a Yong-Min Lee,^b Yeonju Kwak,^a Yoshitaka Yoda,^c Makina Saito,^d Masayuki Kurokuzu,^d Yasuhiro Kobayashi,^d Makoto Seto,^d Lawrence Que, Jr.,^{*e} Wonwoo Nam,^{*b} and Edward I. Solomon^{*af}

^aDepartment of Chemistry, Stanford University, Stanford, California 94305, USA. ^bDepartment of Bioinspired Science, Department of Chemistry and Nano Science, Center for Biomimetic Systems, Ewha Womans University, Seoul 120-750, Korea. ^cSpring-8, JASRI, Hyogo 679-5198, Japan. ^dResearch Reactor Institute, Kyoto University, Osaka 590-0494, Japan. ^eDepartment of Chemistry, University of Minnesota, Minneapolis, Minnesota 55455, USA. ^fSLAC National Accelerator Laboratory, Menlo Park, California 94025, USA.

Supplementary methods:

Resonance Raman Spectroscopy: Resonance Raman spectra were collected using a Spex 1877 CP triple monochromator with an Andor iDus DU420A BR-DD CCD detector. 778nm excitation was provided by a Coherent 890 Ti-Sapphire laser with incident power of 300 mW. A $\sim 135^\circ$ backscattering configuration was used. Data were collected directly on the NRVS sample of **1**, which was cooled to 77K in a liquid N₂ finger dewar.

Supplementary Results and Analysis:

Resonance Raman spectroscopy on solid 1: solvation effect: As discussed in the main text, in acetonitrile, the resonance Raman spectrum of **1** shows a symmetric $\nu\text{Fe-O}_2$ of 493 cm⁻¹, shifting to 478 cm⁻¹ with ¹⁸O substitution (487 shifting to 468 cm⁻¹ in *d*₆-acetone). As shown in Figure 1, NRVS spectroscopy on a powder sample of **1** instead showed an intense band at 434 cm⁻¹, and this was assigned as the symmetric $\nu\text{Fe-O}_2$. To support this assignment, the resonance Raman spectrum of solid **1** was collected. These data, shown in Figure S1, also show a band at 432 cm⁻¹ and no bands in the 460-

520 cm^{-1} region. Solvation thus leads to a $\sim 60 \text{ cm}^{-1}$ shift in the energy of the symmetric $\nu\text{Fe-O}_2$. One possible explanation for this is a structural change in the Fe-O_2 unit upon solvation; however, the Fe-O bond lengths from EXAFS on **1** in solution (1.92 Å) agree closely with those from its crystal structure (1.91 Å).²⁵ To further consider this possibility, we calculated an end-on Fe^{III} -peroxy structure, and found that upon going end-on, an unprotonated Fe^{III} -peroxy changes in electronic structure to have significant high-spin Fe^{II} -superoxy, ferromagnetically coupled character. This leads to a longer Fe-O bond (1.97 Å) and a lower energy $\nu\text{Fe-O}$ (351 cm^{-1}), inconsistent with solution EXAFS^{25,27} and with resonance Raman,^{25,27} respectively, and this structure can be eliminated.

A second possibility is the coordination of a *trans* solvent ligand. Acetonitrile, water, and hydroxide were considered. Of these, only hydroxide stayed bound upon optimization, giving both a side-on and end-on Fe-O_2 structure, with the end-on lower in energy by 5.1 kcal/mol. As with the above structures, the end-on hydroxide-bound complex was found to have significant Fe^{II} -superoxy character with a weak Fe-O bond (2.12 Å, 310 cm^{-1}). The side-on hydroxide-bound structure has a symmetric $\nu\text{Fe-O}_2$ at 471 cm^{-1} , closer to the solution rR value, but the Fe-O bond lengths of 1.96 and 1.97 Å are inconsistent with the solution EXAFS (note that the higher energy of this stretch despite the longer Fe-O bonds relative to the structure without hydroxide bound is due to mixing of the symmetric stretch with the *trans* $\nu\text{Fe-OH}$ at 398 cm^{-1}).

Another possibility is a hydrogen bonding interaction with the Fe-O_2 unit that perturbs the symmetric $\nu\text{Fe-O}_2$ energy. To test this possibility, we computationally added a discrete water (present at a significant amount due to the hydrogen peroxide used in the synthesis) hydrogen bonding to one of the O atoms in the Fe-O_2 unit of our DFT structure of **1** and reoptimized. Structural details for this model are included in Table S2; note that only minimal changes in the structure of the Fe-O_2 unit are found upon adding the water. The calculated energy of the symmetric $\nu\text{Fe-O}_2$ is now mixed over four modes from 469 to 486 cm^{-1} , increased by $40\text{-}57 \text{ cm}^{-1}$ relative to the structure without water (429 cm^{-1}). This

distribution over modes is due to artificial mixing with a water wag; eliminating this mixing by increasing the water proton masses to 100 amu^{51} leads to a single symmetric $\nu\text{Fe-O}_2$ at 472 cm^{-1} . This change in $\nu\text{Fe-O}_2$ energy is not due to changes in the structure of the Fe-O_2 unit arising from the hydrogen bonding interaction, as removing the water, fixing the Fe-O_2 unit, reoptimizing under that constraint, and recalculating the frequencies gave a symmetric $\nu\text{Fe-O}_2$ of 434 cm^{-1} , an energy similar to that found in the freely optimized case without water. Without water, the symmetric stretch has 28% $\nu\text{O-O}$ character, and with water, the stretch has 24% $\nu\text{O-O}$ mixing. The greater mixing with the O-O in the structure without water would lower the energy of the symmetric $\nu\text{Fe-O}_2$. To evaluate whether this change in $\nu\text{Fe-O}_2$ and $\nu\text{O-O}$ mixing could lead to such a significant change in $\nu\text{Fe-O}_2$, we increased the force constant for the O_2 along the O-O stretching vector by 20%. This increases the $\nu\text{O-O}$ energy from 850 to 943 cm^{-1} and leads to a structure with a symmetric $\nu\text{Fe-O}_2$ at 477 cm^{-1} with 23% $\nu\text{O-O}$ mixing. Thus, the hydrogen bond to water decreases the mixing between $\nu\text{Fe-O}_2$ and $\nu\text{O-O}$, leading to a higher energy symmetric stretch. This calculated structure including water is consistent with all the structural and vibrational data for **1** in solution.

Supplementary figures and tables:

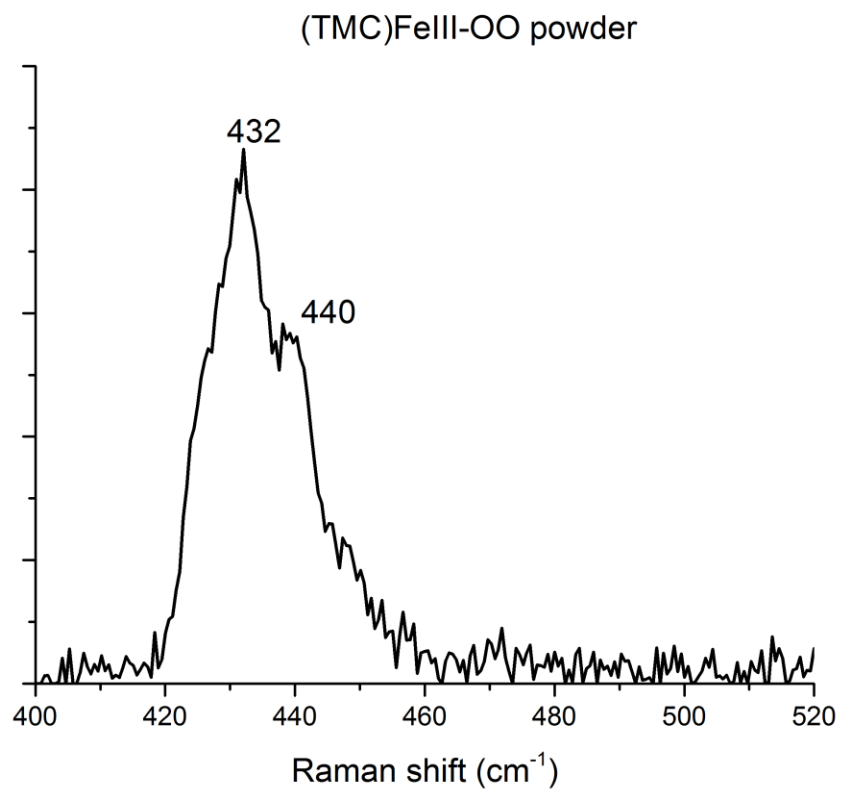


Figure S1. Resonance Raman on solid **1** (excitation: 778 nm)

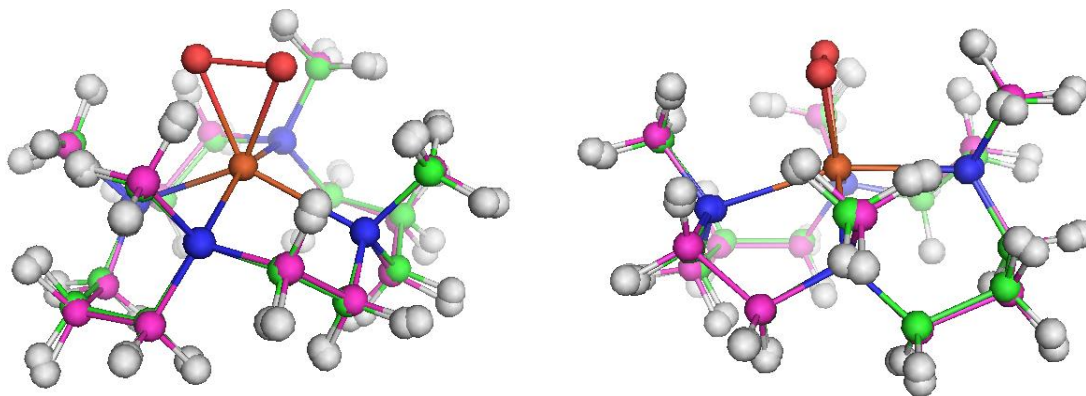


Figure S2. Overlay of crystal structure for **1** (magenta) and DFT-optimized structure (green).

Table S1. Selected bond lengths and angles for the crystal and DFT-optimized structures of **1**.

	Crystal structure	DFT-optimized (no water)	DFT-optimized (water)
Fe-O1 (Å)	1.906	1.924	1.921
Fe-O2 (Å)	1.914	1.925	1.933
Fe-N (ave) (Å)	2.225	2.261	2.261
O-O (Å)	1.463	1.501	1.512
Fe-O1-O2 (°)	67.8	67.0	67.3

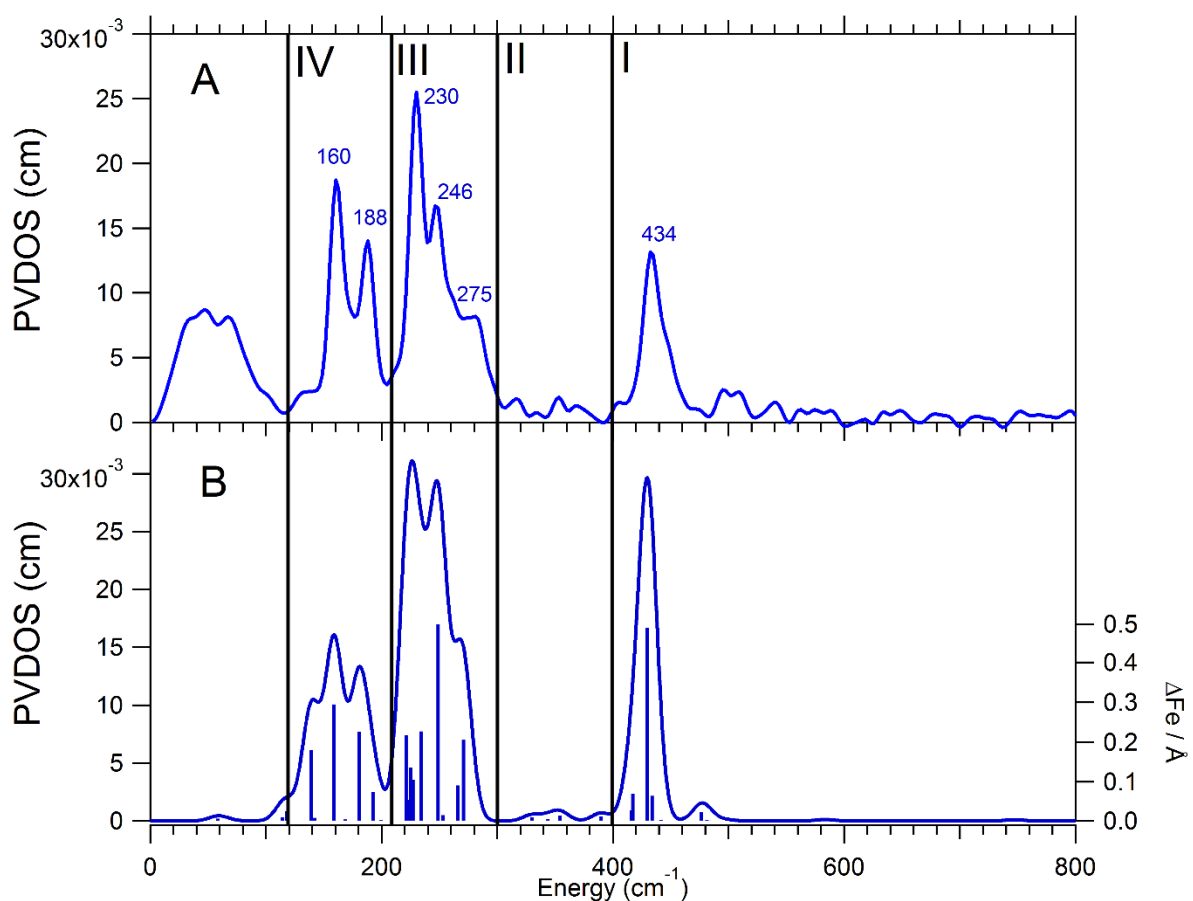


Figure S3. A: NRVs spectrum of **1**. B: Simulated NRVs spectrum for **1** with the Cartesian force constants for the equatorial nitrogen atoms increased by 10%. The relative integrated intensity ratios of the three regions in the simulation remains consistent with experiment, and better intensity agreement within Regions III and IV is found relative to experiment. The calculated shoulder in Region III is now more prominent and correlates well with experiment.

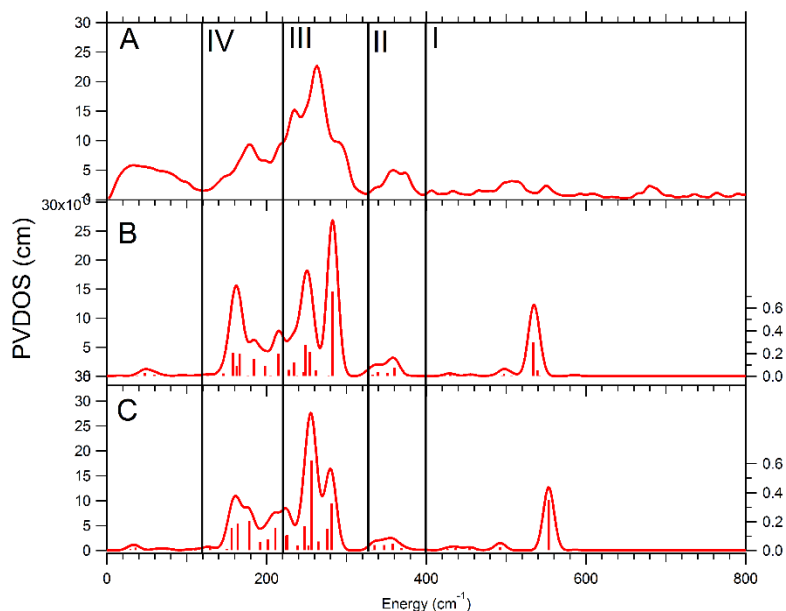


Figure S4. **A:** NRVs spectrum of **2** for comparison. **B:** Initial DFT simulation for **2** with no hydrogen bonding interactions. The region from 150 to 200 cm^{-1} has too much intensity relative to the 220 to 300 cm^{-1} region. **C:** DFT simulation for **2** with one water as an H-bond acceptor from the proton on the distal O. The region from 150 to 200 cm^{-1} has the appropriate amount of intensity, but the $\nu\text{Fe-O}$ is still 100 cm^{-1} too low in energy.

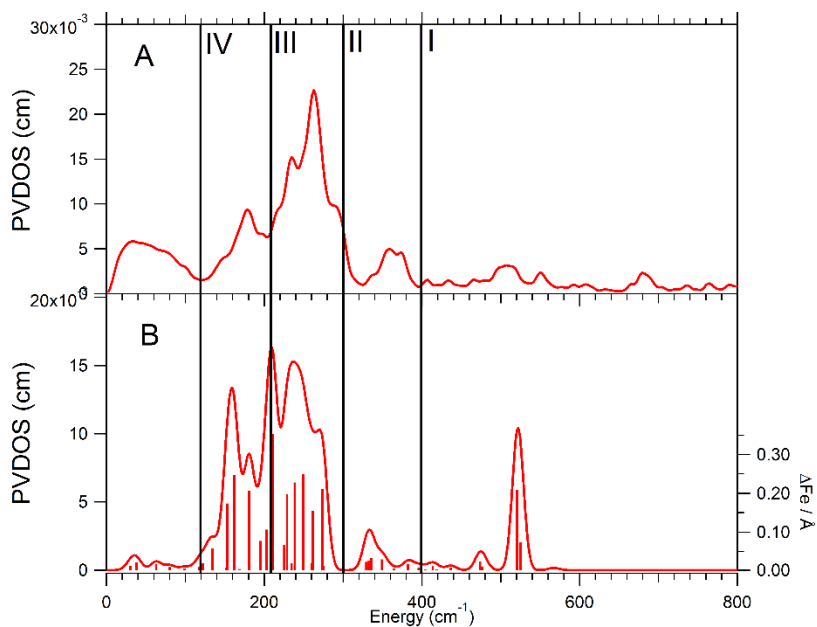


Figure S5. **A:** NRVs spectrum of **2**. **B:** Simulated NRVs spectrum for **2** with water hydrogen bonding to the distal O proton, freely optimized. BP86 underpredicts the Fe-O stretching frequency by 150 cm^{-1} , and additionally gives worse agreement with experiment in Regions III and IV.

Table S2. Calculated structural and vibrational parameters for **2** with water hydrogen bonding to the distal O proton, freely optimized, using the BP86 and B3LYP functionals.

	Fe-O distance (Å)	O-O distance (Å)	Fe-O-O angle (°)	$\nu_{\text{Fe-O}}$ (cm^{-1})	$\nu_{\text{O-O}}$ (cm^{-1})
BP86	1.85	1.48	120.2	521	853
B3LYP	1.83	1.46	121.0	553	877

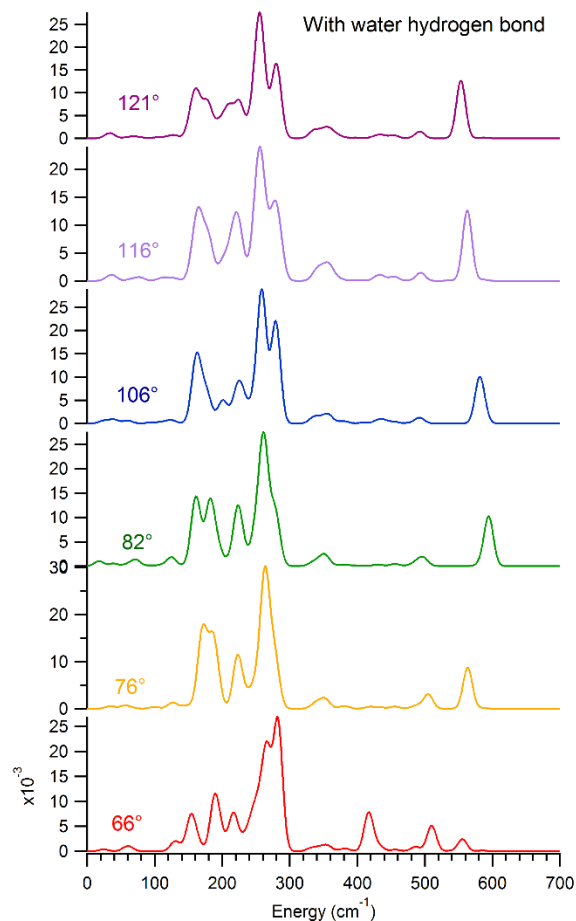


Figure S6. NRVS simulations for Fe-hydroperoxy structures with varying Fe-OO angles, including a water donating a hydrogen bond to the distal O proton. Note that the Fe-O stretch decreases in energy and increases in intensity for structures with an Fe-OO angle greater than 82°, and the intensity pattern in the low-energy region is consistent with the experimental NRVS spectrum of **2** for all structures with an Fe-OO angle of 106° or greater. A previous study also shows changes in a dihedral angle influences band intensities in NRVS simulations.⁵²

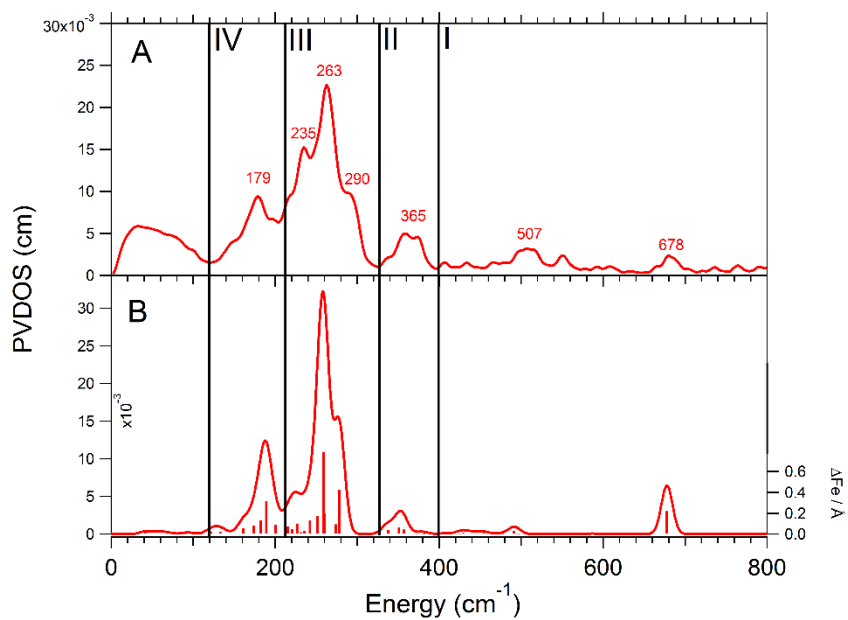


Figure S7. A) NRVS spectrum of **2**. B) NRVS simulation of **2**, with the force constant for the proximal O increased by 25% along the Fe-O vector. The $\nu_{\text{Fe-O}}$ is now at 678 cm^{-1} , in agreement with experiment. In addition, the intensity of the $\nu_{\text{Fe-O}}$ has decreased in better agreement with experiment, and the intensities of the bands in Region III are improved relative to the simulation in Figure 2B.

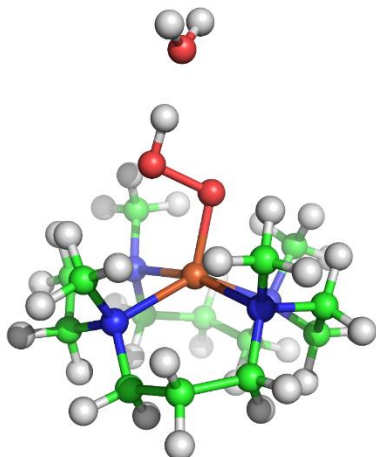


Figure S8. Final optimized structure of **2**.

Table S3. Structural and vibrational information on the side-on peroxy structure (row 1) and distally protonated structures with varying angles, with water accepting a hydrogen bond from the proton. All protonated structures demonstrated mixing of Fe displacement into the $\sim A_1$ and $\sim B_1$ equatorial Fe-ligand stretching modes.

	Fe-L _x distance (Å)	ν Fe-L _x ($\sim E$) (cm ⁻¹)	Fe-L _y distance (Å)	ν Fe-L _y ($\sim E$) (cm ⁻¹)	Fe-O distance (Å)	ν Fe-O (cm ⁻¹)	Fe-OO rock (cm ⁻¹)	Fe-OO bend (cm ⁻¹)
Side-on	2.28	221	2.24	244	1.92, 1.92	430	182	-
66°	2.23	282	2.22	266	1.98, 1.97	510	189	-
76°	2.22	275	2.22	263	1.90	535	186	-
82°	2.21	274	2.22	261	1.88	595	181	-
106°	2.18	279	2.23	259	1.85	581	-	225
116°	2.17	277	2.23	257	1.84	563	-	226
121°	2.17	281	2.22	256	1.83	553	-	229

Supplementary references:

S1. Park, K; Solomon, E. I. *Canadian Journal of Chemistry* **2014**, 92, 975-978.

S2. Galinato, M. G.; Kleingardner, J. G.; Bowman, S. E.; Alp, E. E.; Zhao, J.; Bren, K.L.; Lehnert, N. *Proceedings of the National Academy of Sciences* **2012**, 109, 8896-900.